

Staringite discredited

LEE A. GROAT* AND ANDREW PUTNIS

Department of Earth Sciences, University of Cambridge, Cambridge CB2 3EQ, U.K.

STEPHEN A. KISSIN

Department of Geology, Lakehead University, Thunder Bay, Ontario P7B 5E1, Canada

T. SCOTT ERCIT

Canadian Museum of Nature, Mineral Sciences Section, Ottawa, Ontario K1P 6P4, Canada

FRANK C. HAWTHORNE

Department of Geological Sciences, University of Manitoba, Winnipeg, Manitoba R3T 2N2, Canada

AND

RICHARD V. GAINES

Rt. 1, Box 69, Earlysville, Virginia 22936, U.S.A.

Abstract

Detailed examination of 'staringite' by X-ray precession photography and high-resolution transmission electron microscopy shows it to consist of a sub-microscopic intergrowth of cassiterite and tapiolite. 'Staringite' is discredited as a valid mineral species.

KEYWORDS: staringite, Ta/Nb oxide minerals, pegmatites, transmission electron microscopy

Introduction

STARINGITE was first described from the granitic pegmatite dykes at Seridózinho and Pedro Lavreda, Paraíba State, Brazil (Burke *et al.*, 1969). At this locality, staringite occurs as inclusions in tapiolite. The formula proposed was $(\text{Fe},\text{Mn})_{0.5}(\text{Sn},\text{Ti})_{4.5}(\text{Ta},\text{Nb})_{1.0}\text{O}_{12}$; the mineral was tetragonal and was presumed to have the tri-rutile structure. Since then, staringite has been reported from eastern Siberia (Khvostova *et al.*, 1974) and Kazakhstan (Khvostova *et al.*, 1982). In eastern Siberia, staringite occurs as fine irregular grains in contact with tapiolite and wodginite. In Kazakhstan, it occurs as fine, irregular grains in contact with microlite, columbite and the poorly-characterized phase 'ainalite'.

An occurrence of staringite in the Georgia Lake pegmatite field of northwestern Ontario, Canada, was reported by Zayachkivsky (1985) and Kissin and Zayachkivsky (1985, 1986). The mineral occurs in the core zone of the MNW pegmatite, where it had been previously identified as cassiterite (Breaks, 1980). It is present as anhedral to subhedral grains up to a few centimetres in diameter, containing scattered euhedra of tantalite up to a few hundred micrometres maximum dimension.

Doubts concerning the validity of staringite were expressed by Černý and Ercit (1985). They pointed out that occurrences of staringite and ainalite reported by Khvostova *et al.* (1974, 1982) were identified on the basis of composition and optical and physical properties only. These characteristics, however, are insufficient to distinguish staringite from 'ainalite', and both of these from Ta-bearing cassiterite. During a systematic examination of the Ta/Nb oxide minerals by high-resolution transmission electron microscopy, we

* Present address: Department of Geological Sciences, University of British Columbia, Vancouver, British Columbia V6T 1Z4, Canada



FIG. 1. BSE photograph showing wodginite (medium grey) cut by a vein of tapiolite (white) and cassiterite/ 'staringite' (dark grey); the length of the scale bar is 1 mm.

examined staringite and found it to be a mixture of cassiterite and tapiolite. Accordingly, staringite is discredited as a mineral; this discreditation has been approved by the International Mineralogical Association Commission on New Minerals and Mineral Names.

Samples

Staringite was discovered by Mr Luizelio Barreto of Recife, Brazil. He gave half of the sample to Mrs Maria S. Adusumilli of the University of Recife; this material was used in the original characterization by Burke *et al.* (1969). We obtained the other half of the specimen from Mr Barreto in 1985. A BSE image of this sample is shown in Fig. 1. It consists primarily of wodginite that is cut by a vein of other Ta/Nb-oxide minerals. The vein is a mixture of tapiolite, cassiterite and 'staringite'. The tapiolite forms large optically homogeneous grains, whereas the cassiterite and tapiolite appear optically inhomogeneous.

The Georgia Lake sample (Fig. 2) is highly fractured with some veining by quartz. More significantly, the massive 'staringite' contains semi-coherent masses and stringers of tapiolite of various size.

Experimental

Electron microprobe analysis

Electron-microprobe analyses were done on a JEOL 733 instrument at the Canadian Museum of Nature. Analyses were done in wavelength-dispersion mode with an excitation voltage of 15 kV and sample current of 25 nA; individual elements were collected for 50 s or to 0.5% precision, whichever was arrived at first. The standards used were cassiterite (Sn), rutile (Ti), $MnNb_2O_6$ (Mn, Nb), almandine (Fe), and

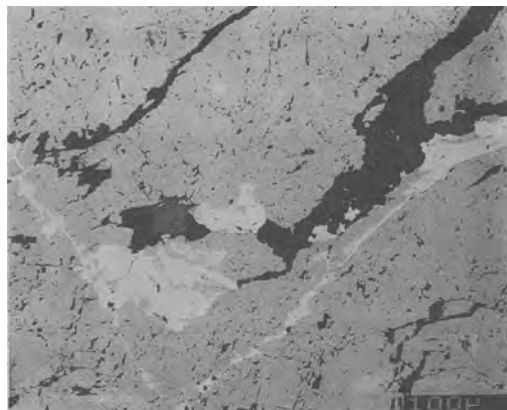


FIG. 2. BSE photograph of 'staringite' from the MNW pegmatite, Georgia Lake pegmatite field. Black areas are voids, some occupied by quartz (dark grey). Semi-coherent exsolution of tapiolite (light grey) is present as irregular masses and veinlets, with some very fine exsolution (lower left).

$NiTa_2O_6$ (Ta). Analyses are given in Tables 1 and 2 where they are compared with 'staringite' analyses from previous studies.

High-resolution transmission electron microscopy (HRTEM)

The 'staringite' sample was examined with a JEOL JEM 100CX 100kV high-resolution transmission electron microscope at the Department of Earth Sciences, University of Cambridge. The material was prepared as a crushed-grain mount suspended on an amorphous carbon grid. Both HRTEM and selected-area diffraction (SAD) images were used to examine the specimen.

Precession photography

Single crystals of 'staringite' were extracted from the electron-microprobe mount of the Brazilian material, mounted on a Buerger precession camera and examined with Zr-filtered $Mo-K\alpha$ X-radiation. The Georgia Lake material was also examined in this fashion.

Results

Electron microprobe analyses

The Brazilian sample consists primarily of 'staringite', tapiolite and Ta-poor 'staringite', the latter occurring in very small amounts throughout

TABLE 1. Chemical analyses of 'staringite'.

	1	2	3	4	5	6	7	8
MnO (wt.%)	0.3	0.15	0.00	2.0	2.3	0.0	0.00	0.00
FeO	3.7	3.62	1.91	-	-	2.8	1.50	0.55
Fe ₂ O ₃	-	-	-	3.1	4.3	-	-	-
TiO ₂	0.03	0.00	0.00	0.3	1.6	0.0	0.00	0.00
SnO ₂	73.3	74.26	87.14	70.0	64.0	76.6	89.42	97.78
Nb ₂ O ₅	1.8	1.35	0.70	1.6	4.6	4.0	1.52	0.00
Ta ₂ O ₅	21.5	19.92	9.87	23.0	22.8	17.1	8.34	1.91
Total	100.6	99.30	99.62	100.0	99.6	100.5	100.78	100.24
Cations per 12 (O)								
Mn ²⁺	0.04	0.02	0.00	0.26	0.29	0.00	0.00	0.00
Fe ²⁺	0.47	0.47	0.24	-	-	0.35	0.19	0.07
Fe ³⁺	-	-	-	0.35	0.48	-	-	-
Ti ⁴⁺	0.00	0.00	0.00	0.03	0.18	0.00	0.00	0.00
Sn ⁴⁺	4.47	4.59	5.31	4.24	3.78	4.61	5.35	5.87
Nb ⁵⁺	0.12	0.09	0.05	0.11	0.31	0.27	0.10	0.00
Ta ⁵⁺	0.89	0.84	0.41	0.95	0.92	0.70	0.34	0.08
	6.00	6.01	6.01	5.95	5.96	5.93	5.98	6.02

1. Type 'staringite', Seridózinho, Brazil (Burke *et al.*, 1969).
2. Type 'staringite', Seridózinho, Brazil — Ta-rich region (this study).
3. Type 'staringite', Seridózinho, Brazil — Ta-poor region (this study).
4. 'Staringite', eastern Siberia, U.S.S.R. (Khvostova *et al.*, 1974).
5. *Ibid.*
6. 'Staringite', Kazakhstan, U.S.S.R. (Khvostova *et al.*, 1982).
7. 'Staringite', Georgia Lake, Ontario — Ta-richest grain (Zayachkivsky, 1985).
8. 'Staringite', Georgia Lake, Ontario — Ta-poorest grain (Zayachkivsky, 1985).

the 'staringite'. The analysis of the 'staringite' given in Table 1 (analysis 2) is virtually identical to that given by Burke *et al.* (1969). Ta-poor 'staringite' has approximately half the amount of Ta, Nb and Fe of 'staringite', with a composition approximately half-way between 'staringite' and ideal cassiterite. 'Staringite' shows a broad range of compositions (Table 1); it is *not* stoichiometric. Ferrotapiolite analyses are given in Table 2, together with the analyses of associated ferrotantalite and ferrowodginitite.

Precession photography

In selecting the crystals used for the precession study, every effort was made to select as homogeneous a fragment of 'staringite' as possible. An $(h0l)$ photograph of the Brazilian sample is shown in Fig. 3. There are strong reflections corresponding to the cassiterite lattice ($a \sim 4.73$, $c \sim 3.18$ Å), and weaker but pronounced reflections that indicate a tripled c -axis and correspond to a tapiolite (or 'staringite')

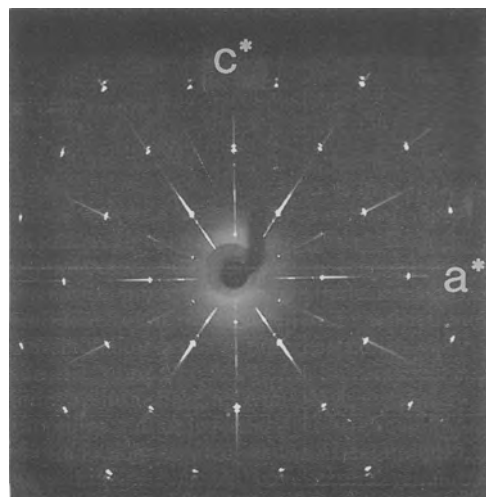


FIG. 3. Zero-level $(h0l)$ precession photograph of 'staringite'; note the splitting of the reflections along $[001]^*$.

TABLE 2. Chemical analyses of oxide minerals associated with type 'staringite'.

	1	2	3	4
*Li ₂ O (wt.%)	-	0.20		
MnO	6.91	3.68	0.69	0.72
FeO	8.73	6.56	13.47	13.41
*Fe ₂ O ₃	-	2.34	-	-
TiO ₂	0.12	0.10	0.00	0.17
SnO ₂	0.16	12.54	0.18	0.55
Nb ₂ O ₅	19.61	9.36	2.90	4.18
Ta ₂ O ₅	64.31	63.12	82.55	79.85
Total	99.84	97.90	99.79	98.88
Cations per unit cell				
Li ⁺	-	0.34	-	-
Mn ²⁺	1.77	1.33	0.10	0.10
Fe ²⁺	2.21	2.33	1.89	1.88
Fe ³⁺	-	0.75	-	-
Ti ⁴⁺	0.03	0.03	0.00	0.02
Sn ⁴⁺	0.02	2.13	0.01	0.04
Nb ⁵⁺	2.68	1.80	0.22	0.32
Ta ⁵⁺	5.29	7.30	3.77	3.64
	12.00	16.00	6.00	6.00
O	24	32	12	12

*For wodginite, Li₂O and Fe²⁺:Fe³⁺ are calculated stoichiometrically (Ercit *et al.*, 1991).

1. Ferrotantalite.
2. Ferrowodginite.
3. Ferrotapiolite (replaced by 'staringite').
4. Ferrotapiolite (exsolution lamella in 'staringite').

lattice ($a \sim 4.73$, $c \sim 9.54$ Å). Careful examination of the reflections with larger l values (e.g. 002, 103) shows a distinct splitting along the c -axis, indicating that the pattern of Fig. 3 consists of two (tetragonal) reciprocal lattices with parallel axes. The superstructure reflections are associated with the larger reciprocal lattice spacing along the c -axis. Thus there are two phases present in the crystal: cassiterite with cell dimensions $a = 4.73$, $c = 3.18$ Å, and an additional phase with cell dimensions $a = 4.73$, $c = 9.23$ Å. These cell dimensions are compatible with the crystal consisting of an intergrowth of cassiterite and tapiolite in the same orientation. The superstructure reflections do not match with the 9.54 Å c -axis proposed by Burke *et al.* (1969). It seems likely that their X-ray powder-diffraction pattern was dominated by the contribution of cassiterite, and the technique lacked the resolution necessary to distinguish the splitting resulting from the difference in the cassiterite and tapiolite substructure c -axes. A reinterpretation of the type diffraction pattern is given in Table 3.

Careful examination of Gandolfi and precession photographs of the Georgia Lake material show the same features as the Brazilian sample, although the distinction of the two reciprocal lattices in precession photographs of the Georgia Lake material is much more subtle than in the Brazilian material. In addition, there is significant smearing along reciprocal-lattice row lines in the Georgia Lake material, indicating that the scale of the intergrowth is much smaller than in the Brazilian material.

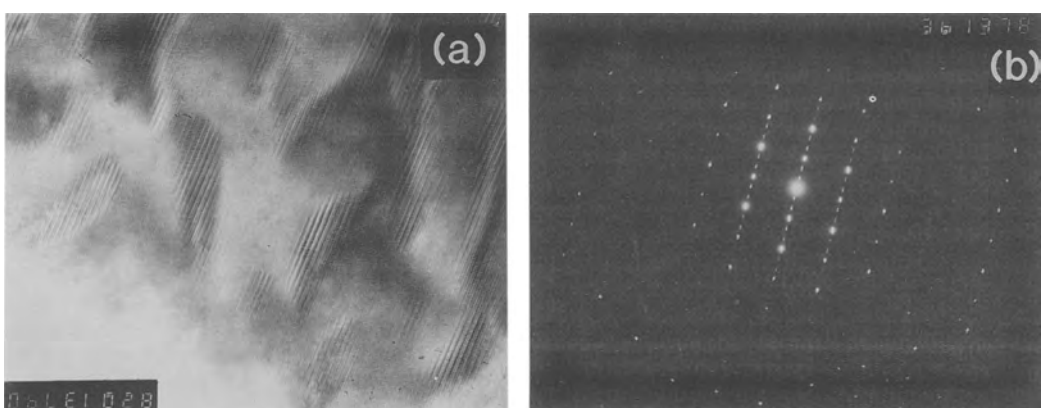


FIG. 4. (a) HRTEM image showing coherent tapiolite domains in cassiterite; (b) SAD pattern showing 9 Å repeat (tapiolite) along [001]* and 3 Å repeat of cassiterite.

TABLE 3. Reinterpretation of the type diffraction pattern for 'staringite'.

1		2		3	
<i>I</i>	<i>d</i>	<i>d</i>	<i>hkl</i>	<i>d</i>	<i>hkl</i>
2	4.75	4.75	002		
3	4.23	4.23	101		
10	3.36	3.36	110		
<1	2.738	2.738	112	3.36	110
8	2.644	2.644	103	2.644	101
4	2.374	2.374	200	2.374	200
1	2.307	2.307	113	2.307	111
<1	2.125	2.125	210	2.125	210
<1	2.070	2.070	211		
9	1.762	1.762	213	1.762	211
4	1.677	1.677	220	1.677	220
2	1.590	1.590	006	1.590	002
4	1.499	1.499	310	1.499	310
4	1.438	1.438	116	1.438	112
4	1.415	1.415	303	1.415	301
2	1.319	1.319	206	1.319	203
4	1.214	1.214	323	1.214	321
1	1.186	1.186	400	1.186	400
3	1.152	1.152	226	1.152	222
1	1.118	1.118	330	1.118	330

1. Type pattern (Burke *et al.*, 1969)2. Tapiolite component: $a = 4.742$, $c = 9.535 \text{ \AA}$ 3. Cassiterite component: $a = 4.742$, $c = 3.178 \text{ \AA}$

HRTEM

Fig. 4*a, b* shows an electron micrograph of the Brazilian material in [010] projection. There are prominent fringes perpendicular to [001] with a spacing of $\sim 3 \text{ \AA}$, corresponding to the cassiterite structure. Intimately intergrown with this in a coherent fashion are areas in which the fringes are associated with triplets of different relative intensities. These are interpreted as domains of tapiolite with the tri-rutile-type structure. From the variation in relative intensities of the fringes in these domains, it seems that, in some cases, the tapiolite is well-ordered, whereas in other domains, the different contrast of the fringes suggests significant cation disorder. However, irrespective of the structural state of the tapiolite, it is clear from Fig. 4*a* that the 'staringite' is actually an intergrowth of cassiterite and tapiolite.

Discussion

The X-ray precession photographs and HRTEM images show 'staringite' to be a sub-microscopic mixture of cassiterite and tapiolite. The texture shown in Fig. 1 suggests that cassiterite is

replacing a vein of tapiolite at high temperatures, when significant Fe, Mn and Ta can be incorporated into the cassiterite structure via solid solution of (disordered) tapiolite. With falling temperature, this homogeneous precursor phase (phase I) decomposed into a coherent intergrowth of tapiolite and phase II, an initially homogeneous phase, in coarse lamellae about 0.5 mm wide and a few millimeters long (Fig. 5*A*). Phase II decomposed to a second generation of tapiolite (tapiolite II) and cassiterite (cassiterite I; Fig. 5*B*). Cassiterite is present as areas apparently free of inclusions, and it seems that this material was originally identified as staringite (Fig. 5*C*). At the highest magnification, it can be seen that cassiterite I has decomposed to an incoherent to semi-coherent intergrowth of low-Ta cassiterite (cassiterite II) and tapiolite III (Fig. 5*D*). This sequence of exsolution is diagrammatically outlined in Fig. 6.

Conclusion

'Staringite' is not a valid mineral species, but an exsolved mixture of cassiterite and tapiolite.

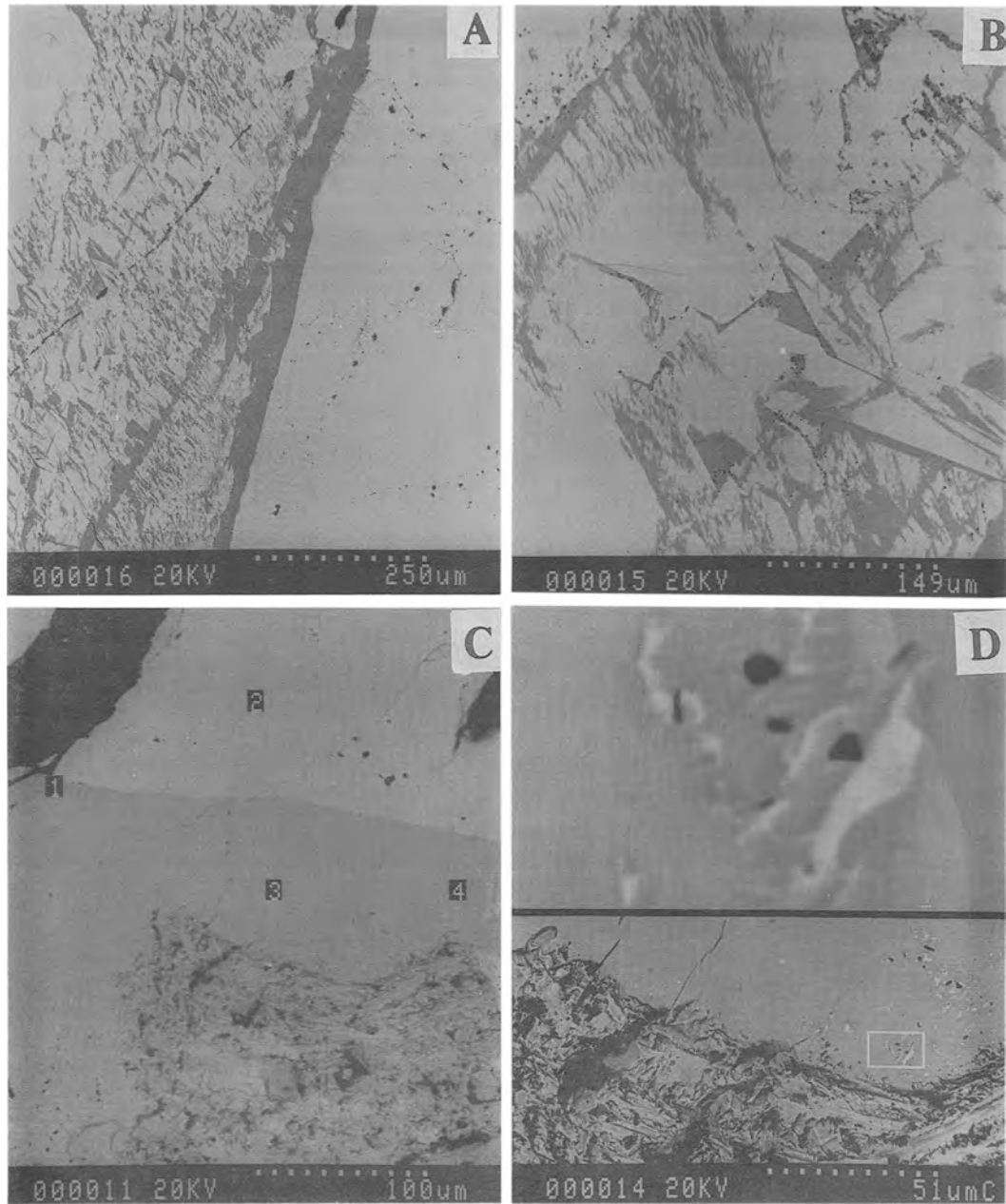


FIG. 5. Holotype 'staringite' from Seridózinho, Paraíba, Brazil. (A) Coarse lamellae of inclusion-free tapiolite I (right) and an apparently homogeneous precursor phase II, now composed of cassiterite I lamellae and veinlets (dark) in a host of tapiolite II. (B) Detail of cassiterite I lamellae (dark) in tapiolite II host. (C) Inclusion free tapiolite II(2) and cassiterite I(1) with a rim (upper left) of cassiterite II(1). Scratch marks in lower centre were made by Burke *et al.* (1969) in obtaining their X-ray specimen. Minute cassiterite II-tapiolite III intergrowths (4) occur in a few places in cassiterite I. (D) Detail of incoherent to semi-coherent intergrowth of cassiterite II (dark) and tapiolite III (light). Black euhedra are quartz.

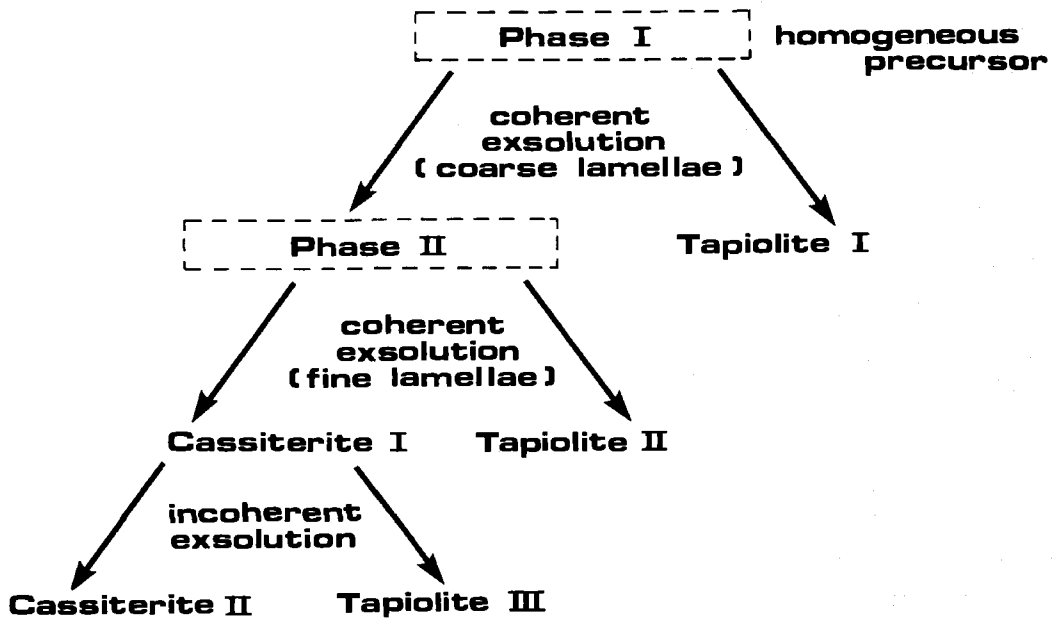


FIG. 6. Sequence of exsolution steps in sample from Seridózinho, Paraiba, Brazil.

Acknowledgements

The authors are grateful to Mr Luizelio Barreto for generously providing the material used in this work. Financial support was provided by the Natural Sciences and Engineering Research Council of Canada in the form of Operating Grants to LAG and FCH, by NATO in the form of a Science Fellowship to LAG, and by the Canadian Museum of Nature in the form of operating funds to TSE.

References

Breaks, F. W. (1980) Lithophile mineralization in northwestern Ontario: rare-element granitoid pegmatites. In *Summary of Field Work 1980* (V. G. Milne, O. L. White, R. B. Barlow, T. A. Robertson and A. C. Colvin, eds.) *Ont. Geol. Surv. Misc. Paper*, **96**, 5–9.

Burke, E. A. J., Kieft, C., Felius, R. O. and Adusumilli, M. S. (1969) Staringite, a new Sn-Ta mineral from north-eastern Brazil. *Mineral. Mag.*, **37**, 447–52.

Černý, P. and Ercit, T. S. (1985) Some recent advances in the mineralogy and geochemistry of Nb and Ta in rare-element granitic pegmatites. *Bull. Mineral.*, **108**, 499–532.

Ercit, T. S., Černý, P., Hawthorne, F. C. and

McCammon, C. A. (1992) The wodginitic group. II. Crystal chemistry. *Can. Mineral.*, **30**, 613–31.

Khvostova, V. A., Slesarchuk, V. S. and Laputina, I. P. (1974) First find of staringite in the Soviet Union. *Trudy Mineral. Muzeya Akad. Sci. S.S.R.*, **23**, 226–8 (in Russian).

Khvostova, V. A., Lebedeva, S. I. and Maksimova, N. V. (1982) Stanniferous tantaloniobates and their typomorphic features. The rare mineral group of tantalumniobates with tin. *Izvestia akad. Nauk S.S.S.R. Ser. Geol.*, **9**, 89–100 (in Russian).

Kissin, S. A. and Zayachkivsky, B. (1985) Genesis of pegmatites in the Quetico Gneiss Belt of north-western Ontario — Rare-element pegmatites and associated pegmatites of the Georgia Lake pegmatite field. In *Geosci. Res. Grant. Prog., Summary of Res. 1984–85, Ont. Geol. Surv. Misc. Pap.*, (Milne, V. G., ed.), **27**, 186–99.

Kissin, S. A. and Zayachkivsky, B. (1986) Staringite confirmed in the Georgia Lake pegmatite field, northwestern Ontario. *Abstracts, G.A.C./M.A.C./C.G.U. Joint Ann. Mtg., Ottawa*, 1986, 90.

Zayachkivsky, B. (1985) *Granitoids and Rare-Element Pegmatites of the Georgia Lake Area, North-western Ontario*. M.Sc. thesis, Lakehead University, Thunder Bay, Ontario.